PHYSICAL REVIEW B

CONDENSED MATTER

THIRD SERIES, VOLUME 46, NUMBER 10 1 SEPTEMBER 1992-II

Kinetics of virtual phase formation during precipitation of ordered intermetallics

Long-Qing Chen* and A. G. Khachaturyan

Department of Materials Science and Engineering, Rutgers University, Piscataway, New Jersey 08855

(Received 23 January 1992)

The kinetics of structural transformations during precipitation of an ordered phase from a disordered matrix is considered for a prototype binary solid solution in two dimensions. A microscopic kinetic computer simulation technique, which describes simultaneously phase separation, ordering, and coarsening, is employed. It is shown that an ordered phase which does not appear in an equilibrium phase diagram (virtual phase) may temporarily appear at intermediate stages of precipitation. The results are rationalized in terms of thermodynamic stability analysis by taking into account kinetic factors. The structures of antiphase domain boundaries (APB's) are discussed and the role of APB's on the transformation kinetics is emphasized.

I. INTRODUCTION

A precipitation reaction is one of the most important solid-state phase transformations which is usually utilized to improve materials properties. It occurs during aging of a single-phase material within a two-phase field of an equilibrium phase diagram. At a given temperature and pressure, a precipitation reaction, like all other structural transformations, is driven by the reduction of the total Gibbs free energy. Any phase state whose free energy is lower than that of an as-quenched disordered phase could, in principle, appear in the transformation kinetics. Those of them which do not appear on the equilibrium phase diagram we will call "virtual phases." Whether or not these intermediate phases form depends on the transformation path predetermined by the geometry of the free-energy surface and diffusion kinetics.

Recently, we proposed a mechanism of virtual-phase formation based on an assumption that its free energy after quenching into the two-phase field of the phase diagram is lower than that of any other phase (including the equilibrium one at the *same concentration*). Its free energy is, of course, higher than that of the equilibrium two-phase mixture.[1] We have studied a simple system with virtual phases, a binary substitutional solid solution with a miscibility gap. It was shown that an isostructural spinodal decomposition within a miscibility gap may be accompanied by the occurrence of a virtual ordered phase which temporarily appears prior to the formation of two equilibrium disordered phases. Although the free energy of the virtual phase is higher than that of the equilibrium two-phase mixture of the disordered phases, it is, nevertheless, lower than that of the initial disordered phase. Therefore, in this case, the virtual phase occurs until the decomposition process, leading to the equilibrium mixture of two disordered phases, starts. Not any transient phase is virtual. For example, the transient $B32$ ordered phase observed in a recent computer simulation study of the kinetics of the $B2 \rightarrow DO_3$ ordering in a model binary alloy[2] is not a virtual phase since its free energy is higher than that of the DO_3 phase at the same concentration.

There are, however, very few alloy systems whose equilibrium phase diagrams exhibit a miscibility gap or just simple ordering. The most common and technologically most important systems have phase diagrams with a two-phase field formed by a mixture of a disordered phase and ordered intermetallics. The kinetics of precipitation of ordered intermetallics is more complicated than that of the isostructural spinodal decomposition. Recent theoretical thermodynamic stability analyses[3-5] and computer-simulation studies of the precipitation kinetics[6-8] have shown that the precipitation of an ordered intermetallic is usually preceded by congruent ordering, resulting in the formation of a single-phase *nonstoichiometric* transient ordered phase. The nonlinear kinetic analysis[6,7] has demonstrated that the decomposition mechanism of the transient nonstoichiometric ordered phase is mainly associated with the antiphase-domain-boundary (APB) instability resulting in the replacement of the APB's by the equilibrium disordered phase films. To our knowledge, however, the possibility of appearance of a virtual ordered phase during the precipitation of an ordered intermetallic resulting in an equilibrium two-phase mixture has never been discussed. The investigation of the precipitation kinetics of an ordered intermetallic phase involving the virtual-ordered-phase formation is the main purpose of this paper.

In the following section, the computer-simulation tech-

nique employed in this work will be briefly reviewed. Then the kinetics of structural phase transformations, particularly, the formation of a virtual ordered phase during the precipitation of an ordered intermetallic from a disordered matrix in a model binary substitutional solid solution, will be investigated. The kinetics predicted by the computer simulation is then discussed using the thermodynamic stability analysis. And finally, the main results of this paper will be summarized.

II. COMPUTER MODELING OF PHASE SEPARATION AND ORDERING

A standard approach to the thermodynamics and kinetics of a phase transformation is, usually, based on *a priori* assumptions concerning the atomic structures of phases involved. Such an approach has a serious disadvantage since it, in principle, cannot address the problem of transient phases whose structure may be different from those *a priori* assumed. The computer-simulation technique employed in this study, however, does not have this limitation. The only input to the computer simulation is the interatomic interaction potentials. The computer simulation automatically produces crystallographic structures of various possible ordered phases and their morphologies. It is based on the microscopic diffusion theory formulated in reciprocal space:[6,9]

$$\frac{d\tilde{n}(\mathbf{k},t)}{dt}=\tilde{L}_0(\mathbf{k})\frac{\delta F}{\delta\tilde{n}(\mathbf{k},t)} , \tag{1}$$

where $\tilde{n}(\mathbf{k},t)$, $\tilde{L}_0(\mathbf{k})$, and $\delta F/\delta\tilde{n}(\mathbf{k},t)$ are the Fourier transforms of $n(\mathbf{r},t)$ (the occupation probability of a solute atom at the site $\mathbf{r}$ at time t), $L_0(\mathbf{r})$ (the kinetic coefficients proportional to the elementary jump probability at a time unit), and $\delta F/\delta n(\mathbf{r},t)$ (the thermodynamic driving force), respectively, and F is the total free-energy functional of the occupation probabilities.

For a system of N lattice sites, the solution of Eq. (1) gives the time dependence of N concentration wave amplitudes $\tilde{n}(\mathbf{k},t)$, whose back Fourier transform completely determines the microscopic and mesoscale structures of an alloy. If we assume that nonvanishing amplitudes are only at $\mathbf{k}$ close to zero, Eq. (1) is reduced to its continuum limit, the conventional Cahn-Hilliard equation describing the isostructural decomposition.[10] Equation (1) is, however, more general. It describes the evolution of the entire spectrum of concentration waves irrespective of the wavelengths and, particularly, it describes ordering. Ordering is manifested by a spontaneous increase in amplitudes of a concentration wave packet with $\mathbf{k}$ around the superlattice vector of an ordered phase $\mathbf{k}_0$, whereas all other amplitudes vanish. Therefore Eq. (1) describes not only the growth of macroscopic compositional heterogeneities typical for the isostructural spinodal decomposition, but also the development of microscopic atomic-scale heterogeneities characterizing ordering. In principle, the Ginzburg-Landau kinetic equations employed in Refs. 7 and 8 may be obtained from Eq. (1) by the limit transitions to $\mathbf{k}=0$ and $\mathbf{k}=\mathbf{k}_0$. Equation (1) actually describes a wide variety of processes such as atomic ordering, clustering, migration of APB's, and coarsening. It automatically provides ordered structures, either transient or equilibrium, as well as the alloy morphology.

To predict the correct sequence of structural transformations, we do not need a very accurate free-energy functional F. It is just sufficient to have a free energy whose geometry in the coordinate plane of composition and long-range order (LRO) parameters would provide a phase diagram with a two-phase field consisting of ordered and disordered phases. Particularly, we utilize the mean-field free energy

$$F=\tfrac{1}{2}\sum_{\mathbf{r}'\mathbf{r}''}W(\mathbf{r}'-\mathbf{r}'')n(\mathbf{r}')n(\mathbf{r}'')+k_BT\sum_{\mathbf{r}'}\{n(\mathbf{r}')\ln n(\mathbf{r}')+[1-n(\mathbf{r}')]\ln[1-n(\mathbf{r}')]\} , \tag{2}$$

where $W(\mathbf{r}-\mathbf{r}')$ are the interaction energies between atoms at the lattice sites $\mathbf{r}$ and $\mathbf{r}'$, k_B is the Boltzmann constant, and T is the temperature. It is easy to show that the driving force $\delta F/\delta\tilde{n}(\mathbf{k},t)$ in (1) is given by

$$\frac{\delta F}{\delta\tilde{n}(\mathbf{k})}=V(\mathbf{k})\tilde{n}(\mathbf{k})+k_BT\left\{\ln\left[\frac{n(r)}{1-n(r)}\right]\right\}_{\mathbf{k}} , \tag{3}$$

where

$$V(\mathbf{k}) \quad \text{and} \quad \left\{\ln\left[\frac{n(r)}{1-n(r)}\right]\right\}_{\mathbf{k}}$$

are the Fourier transforms of the interchange energies $W(\mathbf{r})$ and $\ln\{n(r)/[1-n(r)]\}$, respectively.

In the computer simulation, Eq. (1) is numerically solved with respect to amplitudes $\tilde{n}(\mathbf{k},t)$ using the Euler technique. More details of the computer-simulation technique may be found in Ref. 6. The real-space atomic distribution $n(\mathbf{r},t)$ is obtained by the back Fourier transform of $\tilde{n}(\mathbf{k},t)$.

III. COMPUTER-SIMULATION RESULTS

To study the decomposition kinetics of a disordered solid solution into a two-phase mixture of ordered and disordered phases and, particularly, the effect of a transient virtual ordered phase on the kinetics, a simple generic binary alloy system in a two-dimensional (2D) square lattice is employed. The thermodynamic characteristics of the 2D model system can be easily determined by using the method of static concentration waves.[11] In this method any ordered phase is described by a superposition of static concentration waves. According to it, the structure of the most stable ordered phase (superstructure) is generated by the ordering wave vector $\mathbf{k}$, which provides the absolute minimum of $V(\mathbf{k})$. For a three-neighbor interaction model in a 2D square lattice, $V(\mathbf{k})$ is given by the equation

$$V(\mathbf{k})=2w_1[\cos2\pi h+\cos2\pi l]+4w_2\cos2\pi h\cos2\pi l+2w_3[\cos4\pi h+\cos4\pi l] , \tag{4}$$

where $\mathbf{k}$ is the reciprocal-lattice vector, and h and l are defined in $\mathbf{k}=(2\pi/a)(h,l)$. Let us consider a specific set of interaction parameters:

$$w_1=-0.25\ ,\quad w_2=1.0\ ,\quad w_3=-1.0\ , \tag{5}$$

where w_1, w_2, and w_3 are the effective interchange energies between first-, second-, and third-nearest-neighbor sites, respectively. The interchange energies as well as all other physical values in the computer simulation are expressed in reduced variables. It is emphasized that any other choice of the interchange energy parameters which provides a similar type of the free-energy dependence on the composition and LRO parameter would result in a similar transformation kinetics.

The minimum of $V(\mathbf{k})$, the Fourier transform of the set of interchange energies (5), falls at $\mathbf{k}$ vectors $(2\pi/a)(\frac{1}{2},0)$ and $(2\pi/a)(0,\frac{1}{2})$, belonging to the same star, with a being the lattice parameter of the square lattice. Since the minimum of $V(\mathbf{k})$ is located at $\mathbf{k}\neq 0$, the system undergoes ordering at low tempertures. The ordered structure is generated by the superlattice vector $\mathbf{k}_{01}=(2\pi/a)(\frac{1}{2},0)$ or $\mathbf{k}_{02}=(2\pi/a)(0,\frac{1}{2})$. These are two orientation variants of the ordered phase β generated by $\mathbf{k}_0$ star $\{\frac{1}{2},0\}$ and described by

$$\begin{aligned} n(\mathbf{r})&=c+c\eta\cos\mathbf{k}_{01}\cdot\mathbf{r}=c+c\eta\cos\pi l\ ,\\ n(\mathbf{r})&=c+c\eta\cos\mathbf{k}_{02}\cdot\mathbf{r}=c+c\eta\cos\pi m\ , \end{aligned} \tag{6}$$

where c is the average composition of the system, η is the LRO parameter, and l and m are the integer coordinates

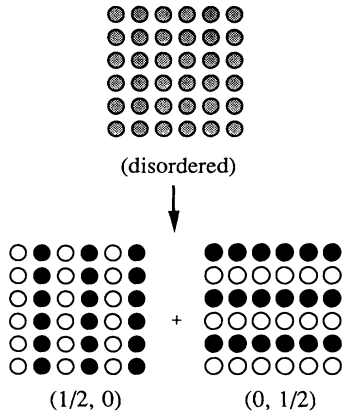

FIG. 1. Structures of a disordered state and two orientation variations of an ordered phase in a two-dimensional square lattice. $n(r)=1.0$ (solid circle), $n(r)=0.0$ (open circle), and $n(r)=0.5$ (grey circle).

along the [1 0] and [0 1] directions defining the crystal-lattice site vectors $\mathbf{r}=l\mathbf{a}_1+m\mathbf{a}_2$, $\mathbf{a}_1$ and $\mathbf{a}_2$ are the unit-cell vectors in real space, $|\mathbf{a}_1|=|\mathbf{a}_2|=a$. The structures of the disordered phase as well as the two variants of the ordered phase are illustrated in Fig. 1.

To calculate the equilibrium phase diagram of the model system, we have to calculate the free energies of the disordered and ordered β phases. To do this we should substitute (6) into (2). It gives

$$\begin{aligned} F(c,\eta,T)=&N\frac{c^2}{2}V(0)+\frac{N}{2}V(\mathbf{k}_0)(c\eta)^2\\ &+N\frac{k_BT}{2}[(c+c\eta)\ln(c+c\eta)+(1-c-c\eta)\ln(1-c-c\eta)+(c-c\eta)\ln(c-c\eta)+(1-c+c\eta)\ln(1-c+c\eta)]\ , \end{aligned} \tag{7}$$

where $V(0)$ is the value of $V(\mathbf{k})$ at $\mathbf{k}$ equal to zero and $V(\mathbf{k}_0)$ is the value of $V(\mathbf{k})$ at $\mathbf{k}_{01}$ or $\mathbf{k}_{02}$. When $\eta=0$, Eq. (7) automatically describes the free energy of the disordered phase. For convenience, Eq. (7) is rewritten in the reduced form

$$\begin{aligned} f(c,\eta,T^*)^*=&\frac{F(c,\eta,T)}{N|V(\mathbf{k}_0)|}\\ =&\frac{c^2}{2}V^*(0)-\frac{1}{2}(c\eta)^2+\frac{T^*}{2}[(c+c\eta)\ln(c+c\eta)+(1-c-c\eta)\ln(1-c-c\eta)+(c-c\eta)\ln(c-c\eta)\\ &+(1-c+c\eta)\ln(1-c+c\eta)]\ , \end{aligned} \tag{8}$$

where $|V(\mathbf{k}_0)|$ is the absolute value of $V(\mathbf{k}_0)$, $V^*(0)=V(0)/|V(\mathbf{k}_0)|$, and T^* is the reduced temperature defined by $T^*=k_BT/|V(\mathbf{k}_0)|$. Using the common-tangent construction, the equilibrium phase diagram calculated from this free-energy model is given in Fig. 2. It is shown in Fig. 2 that aging the disordered phase of low temperatures will result in the precipitation of the ordered intermetallic phase. The ground state of the system at the chosen interaction parameters is the two-phase mixture of the pure A and the ordered phase β for the solute compositions of B between 0 and 0.5, whereas it is the mixture of the pure B and β for the compositions between 0.5 and 1.0.

For the 2D square lattice, the kinetic coefficients $\tilde{L}_0(\mathbf{k})$ in (1) were obtained by assuming that $L_0(\mathbf{r})$ vanishes beyond the nearest-neighbor sites and by using the requirement $\tilde{L}(0)=0$, which follows from the atom-number-conservation condition

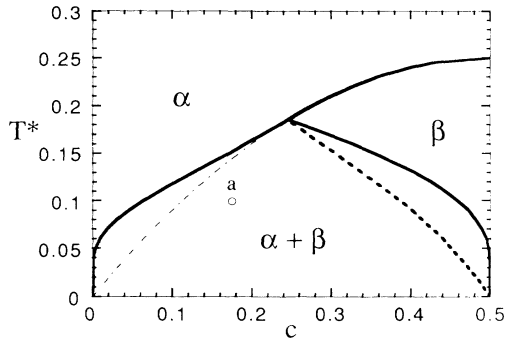

FIG. 2. Phase diagram for a prototype system with a three-neighbor interaction model. T^* is the reduced temperature, and c is the solute concentration. α and β represent the disordered and ordered phases, respectively. The thick lines are phase boundaries. The dot-dashed line is the order-disorder transformation line within the two-phase field as well as the spinodal line of the ordered phase. The dotted line is the other spinodal line of the ordered phase. Point a is the position at which the alloy was aged.

$$\tilde{L}_0(\mathbf{k}) = \sum_{\mathbf{r}} L(\mathbf{r}) e^{i\mathbf{k}\cdot\mathbf{r}} = -4L_1 \left[\sin^2 \frac{\mathbf{k}\cdot\mathbf{a}_1}{2} + \sin^2 \frac{\mathbf{k}\cdot\mathbf{a}_2}{2} \right] = -4L_1 [\sin^2 \pi h + \sin^2 \pi l] , \quad (9)$$

where L_1 is the kinetic coefficient proportional to the reciprocal expectation time of the elementary diffusion jump between the nearest-neighbor sites. The time in the simulation results is presented using the dimensionless reduced time t^*, which is measured in terms of the typical time of an elementary diffusion event, $\tau = 1/L_1|V(\mathbf{k}_0)|$.

The typical temporal structural and morphological transformation during aging of a quenched disordered phase within the two-phase field of the phase diagram (Fig. 2) is illustrated in Fig. 3. Plotted in Fig. 3 are actually the occupation probabilities $n(\mathbf{r},t)$ at each lattice site, represented by different grey levels. Those occupation probabilities were obtained by back Fourier transforming the concentration wave amplitudes $\tilde{n}(\mathbf{k},t)$, which are the solutions of the reciprocal-space equation (1). The corresponding diffraction pattern is shown in Fig. 4. It is presented in terms of $\ln[I(\mathbf{k},t)]$, where $I(\mathbf{k},t)$ is the intensity. The average composition of the alloy is 0.175. The alloy is aged at the temperature $T^* = 0.10$ (point a in Fig. 2).

The initial quenched alloy is simulated by the distribution $n(\mathbf{r},0) = c + \delta c(\mathbf{r})$, where $\delta c(\mathbf{r})$ are the small random perturbations to the average composition c. As expected from our previous studies,[6] the first process which occurs during aging is a congruent ordering. This ordering results in appearance of two orientation variants of ordered modulations related to $\mathbf{k}_{01} = (2\pi/a)(\frac{1}{2},0)$ and $\mathbf{k}_{02} = (2\pi/a)(0,\frac{1}{2})$ [Fig. 3(a), $t^* = 4.0$]. At time $t^* = 15.0$ [Fig. 3(b)], an ordered single phase is formed. In the diffraction pattern [Fig. 4(a)], ordering is manifested by the growth of the concentration wave not only at and around $\mathbf{k} = \mathbf{k}_{01}$ and $\mathbf{k}_{02}$, which are the superlattice vectors of the equilibrium ordered phase, but also at and around $\mathbf{k} = \mathbf{k}_1 = (2\pi/a)(\frac{1}{2},\frac{1}{2})$. This ordered phase formed has the structure shown in Fig. 5, which differs from the structure of the equilibrium ordered phase presented in Fig. 1. Therefore, it is a virtual ordered phase. It is very interesting that the APB's of the virtual ordered phase in Fig. 3(b) are ordered with the structure of the equilibrium ordered phase. A careful examination of the local compositions has shown that the compositional inhomogeneities in the virtual ordered phase state exist because of the solute depletion at the APB's during the growth of the ordered domains.

The ordering which results in appearance of the virtual phase is followed by its decomposition into an equilibri-

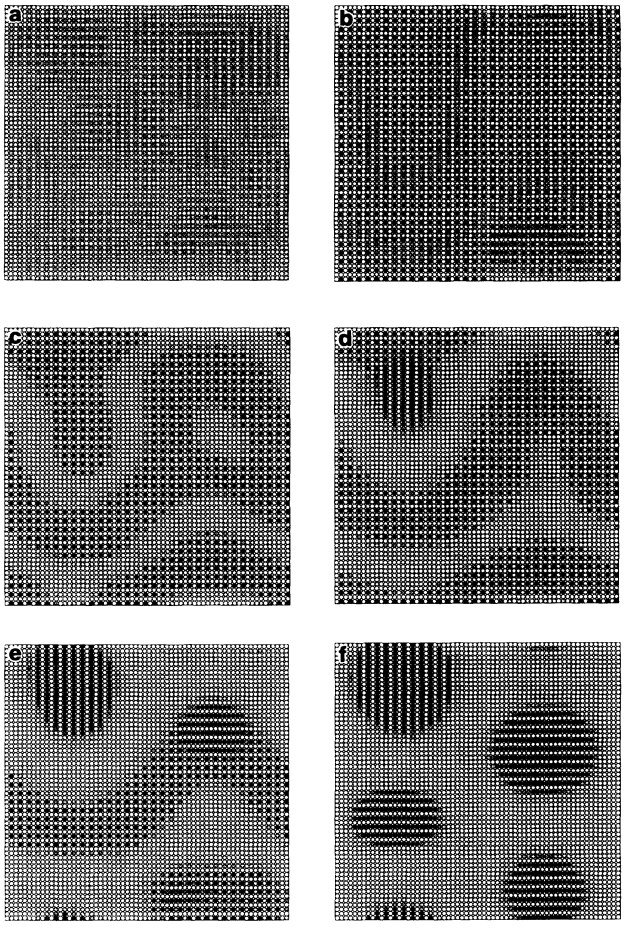

FIG. 3. Temporal evolution of the atomic structures and morphologies for a disordered solution of composition 0.175 aged at the temperature $T^* = 0.10$ within the equilibrium two-phase field at different reduced time t^*. Each picture is a $64a \times 64a$ supercell. The grey levels of the circles represent the occupation probabilities of solute atoms at each lattice site. Complete dark means that the occupation probability is 1.0, while the complete bright means that the occupation probability is 0. All the intermediate grey levels indicate the occupation probabilities between 0 and 1. (a) $t^* = 4.0$, (b) $t^* = 15.0$, (c) $t^* = 100.0$, (d) $t^* = 300.0$, (e) $t^* = 500.0$, and (f) $t^* = 950.0$.

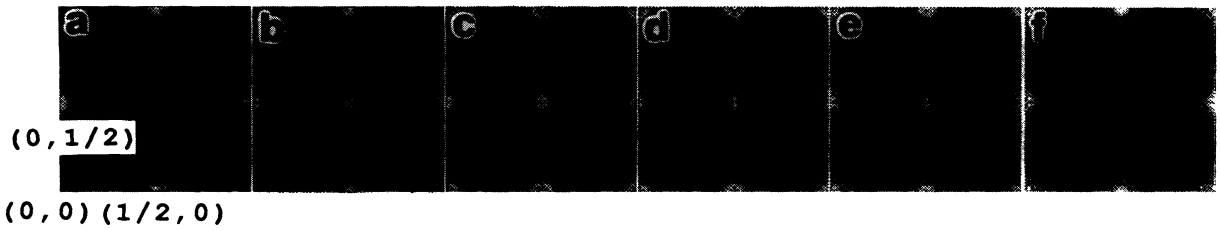

FIG. 4. Temporal evolution of the diffraction intensities within the first Brillouin zone calculated from the atomic structures presented in Fig. 3. Intensities of superlattice reflections are represented by the brightness, with the intensity of the fundamental reflection at the reciprocal-lattice origin (0,0) omitted.

um mixture of stable ordered and disordered phases. Decomposition results in a decrease in the composition of APB regions and an increase in the composition of virtual ordered domains. As shown in Fig. 3(c) for time $t^*=100.0$, the APB's have been replaced by a larger region of the ordered phase with structure of the equilibrium ordered phase and its composition close to the equilibrium disordered phase. Because the composition of the stable ordered phase decreases, its degree of order also decreases [Fig. 3(c)]. At time $t^*=300.0$ shown in Fig. 3(d), the solute deficient ordered phase has become disordered. At one region of the solute-rich virtual ordered phase, it transforms to the equilibrium ordered phase. By the time $t^*=500.0$, more decomposition has taken place, which results in a larger volume fraction of the disordered phase and another region of the virtual ordered phase transforming into the equilibrium ordered phase [Fig. 3(e)]. At time $t^*=950$, as shown in Fig. 3(f), all the virtual ordered phase disappears and a mixture of stable ordered phase and the disordered phase resulted. We can see in Fig. 3(f) both orientation variants of the stable ordered phase, which are embedded in the disordered matrix. Figure 4(f) shows diffraction intensities corresponding to the structure in Fig. 3(f). It demonstrates that the diffuse maximum at the $(2\pi/a)(\frac{1}{2},\frac{1}{2})$ point related to the superlattice point of the virtual phase disappears. The compositions and amount of the ordered and disordered phases are consistent with the equilibrium phase diagram shown in Fig. 2.

IV. DISCUSSION

Our kinetic study has demonstrated that, at a certain geometry of the free-energy surface, a virtual ordered phase may temporarily appear during the decomposition of a disordered phase into a mixture of ordered and disordered phases. The atomic structure of the virtual ordered phase differs from that of the stable ordered phase. The overall structural and morphological transformation kinetics is very different from the case where no virtual ordered phase is involved.[6]

The structure of the virtual ordered phase obtained from the above computer simulation (Fig. 5) may be described by superlattice vectors $\mathbf{k}_0$ and $\mathbf{k}_1$ belonging to two different stars $(2\pi/a)\{\frac{1}{2},0\}$ and $(2\pi/a)\{\frac{1}{2},\frac{1}{2}\}$. According to the concentration-wave method, the virtual ordered phase is described by

$$n(\mathbf{r})=c+c\eta_1[\cos\mathbf{k}_{01}\mathbf{r}+\cos\mathbf{k}_{02}\mathbf{r}]+c\eta_2\cos\mathbf{k}_1\mathbf{r}$$
$$=c+c\eta_1[\cos\pi n+\cos\pi m]+c\eta_2\cos\pi(n+m)\ , \quad (10)$$

where η_1 is the LRO parameter for the concentration wave related to the star $(2\pi/a)\{\frac{1}{2},0\}$ and η_2 is the LRO parameter for the concentration wave related to the vector $(2\pi/a)(\frac{1}{2},\frac{1}{2})$.

The appearance of the virtual ordered phase during precipitation of the equilibrium ordered intermetallic can be rationalized in terms of thermodynamics combined with kinetic factors. The free energies of the disordered phase, the equilibrium ordered phase (6), and the virtual phase (10) are plotted together in Fig. 6. From Fig. 6 we can see that the free energy of the virtual phase (dotted

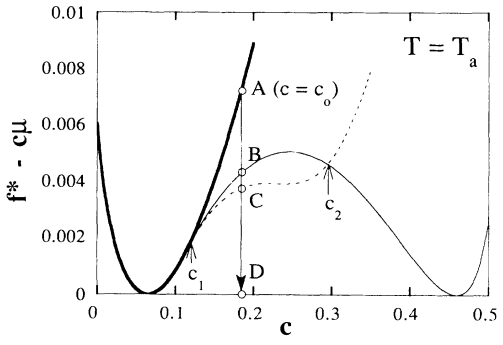

FIG. 6. Free energies of phases involved in the structural transformation. The thick, thin, and dotted lines are the free energies of the disordered, equilibrium ordered, and virtual ordered phases, respectively. f^* is the free energy in reduced unit, c is the solute concentration, and μ is the chemical potential at the equilibrium composition at the aging temperature T_a.

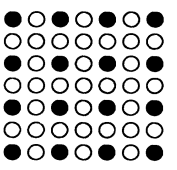

FIG. 5. Structure of the virtual ordered phase.

line) is higher than that of a mixture of equilibrium ordered and disordered phases at all compositions (the common tangent line). However, a segment of the free-energy curve (between compositions c_1 and c_2) lies below both, the disordered phase (thick line) and the equilibrium ordered phase (thin line). Therefore a phase described by this segment meets all requirements to be a virtual phase.[1]

As follows from Fig. 6, during aging of a quenched disordered solution with a composition within the range c_1 and c_2, a virtual ordered single phase is expected to temporarily appear prior to the formation of a mixture of equilibrium phases. For example, if a disordered solid solution with a composition c_0 is quenched into a two-phase field, its free energy is represented by the point A in Fig. 6. The disordered solution can reduce its free energy by two types of ordering, either by ordering producing a transient nonstoichiometric ordered phase whose structure is that of the equilibrium ordered phase (point B) or by ordering producing a virtual ordered phase (point C). Finally, it can reduce its free energy by decomposing into a mixture of equilibrium ordered and disordered phases (point D). For kinetic reasons the first stage will be an ordering transition, producing a non-stoichiometric ordered phase (either B or C). Since point C, corresponding to the virtual phase, is below point B, the virtual phase is stable until a slower process, the decomposition, starts to develop (the computer-simulated kinetics has proved that this is the case). Even if the ordering kinetics of the β phase were faster and, thus, it forms first (the point B), the further free-energy reduction would result in the formation of the more stable virtual phase corresponding to point C. Therefore the virtual ordered phase will always temporarily appear for this particular composition and temperature. This ordering stage will then be followed by the slow decomposition of the congruently ordered virtual phase into the equilibrium ordered phase and the equilibrium disordered phase. This is consistent with our computer-simulation results presented above for the composition $c=0.175$.

When the same thermodynamic stability analysis is applied to systems with a composition greater than c_2, we arrive at a conclusion that congruent ordering would produce an ordered single phase with the structure of the equilibrium ordered phase instead of the virtual ordered phase. This is confirmed in our computer simulation study shown in Fig. 7. In this case, however, our com-

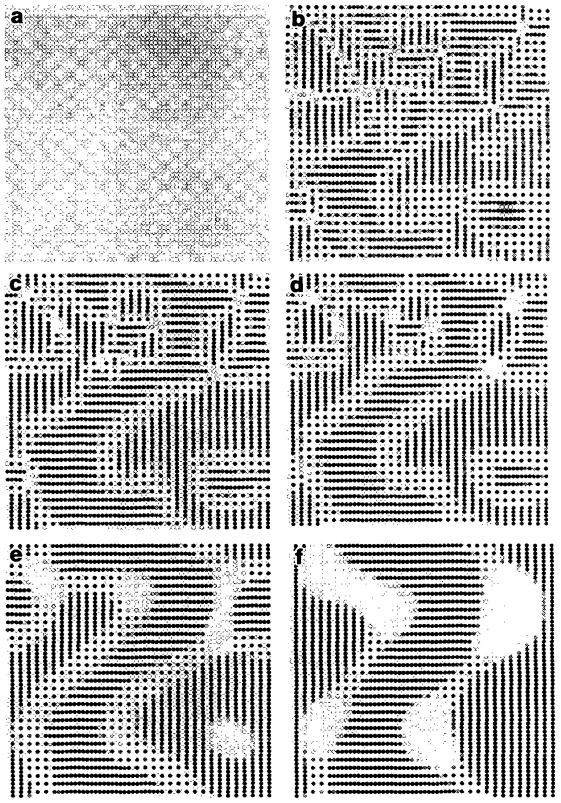

FIG. 7. Temporal evolution of the atomic structures and morphologies for a disordered solution of composition 0.35 aged at the temperature $T^*=0.10$ within the equilibrium two-phase field. (a) $t^*=2.0$, (b) $t^*=5.0$, (c) $t^*=50.0$, (d) $t^*=100.0$, (e) $t^*=305.0$, and (f) $t^*=605.0$.

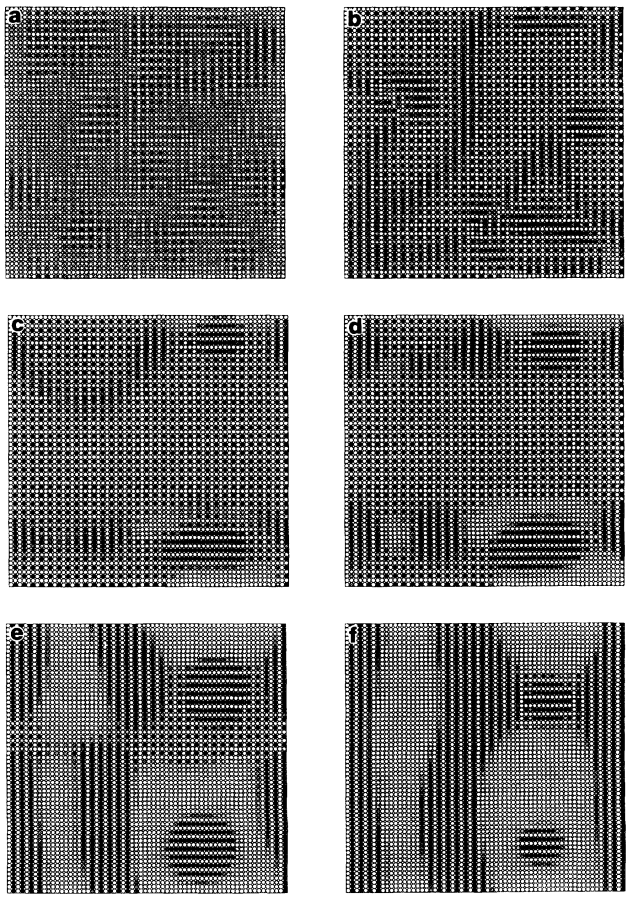

FIG. 8. Temporal evolution of the atomic structures and morphologies for a disordered solution with a composition corresponding to the stoichiometric composition of the virtual ordered phase, aged at the temperature $T^*=0.10$ within the equilibrium two-phase field. (a) $t^*=1.0$, (b) $t^*=2.0$, (c) $t^*=5.0$, (d) $t^*=10.0$, (e) $t^*=50.0$, and (f) $t^*=300.0$.

puter simulation reveals that the boundaries between different orientation domains of the equilibrium ordered phase are wetted by the virtual ordered phase. This virtual ordered phase disappears when the boundaries (APB's and boundaries between orientation domains) are replaced by the equilibrium disordered phase during the decomposition of the congruently ordered single phase.

Finally, from Fig. 5, we can easily determine the stoichiometric composition of the virtual ordered phase, which is 0.25. It is interesting to investigate the structural and morphological transformations when a disordered solution with this stoichiometric composition is aged within the two-phase field ($T^*=0.10$). The temporal evolution during aging is shown in Fig. 8. The overall structural and morphological transformations in this case are quite similar to the case of $c=0.175$, which is nonstoichiometric to the virtual phase. There is, however, one very interesting observation: The decomposition of the virtual phase occurs entirely along the APB's, resulting in the replacement of APB's by both equilibrium disordered and equilibrium ordered phases. Later, regions of both the equilibrium phases expand and the virtual phase gradually disappears.

It is emphasized that the kinetic results obtained in this study are general in the sense that if the free energy of any real alloy system has the similar type of dependence on composition and LRO parameter to that assumed in this paper, the kinetics of decomposition would be the same as predicted in our computer simulation. The obtained results may be even applied to structural transformations where the role of a LRO parameter is played by a displacement (or strain) mode. In this case all conclusions drawn above for ordering could be applied since the displacements generating the congruent formation of the virtual phase are established much faster than the decomposition process producing the equilibrium two-phase mixture.

V. CONCLUSION

Through a computer simulation, a virtual ordered phase was found to appear temporarily during the decomposition kinetics of a disordered phase into a mixture of ordered and disordered phases. The virtual ordered phase is different from the equilibrium ordered phase not only in composition, but in structure as well. The only thermodynamic requirement is that its free-energy curve have a segment which is below those of both equilibrium disordered and ordered phases at the same composition. Finally, the decomposition reactions at APB's are predicted.

ACKNOWLEDGMENTS

This research is supported by the National Science Foundation under Grant No. NSF-DMR-88-17922. The computer simulation was performed on a Cray-YMP at the Pittsburgh Supercomputing Center.

*Present address: Department of Materials Science and Engineering, Pennsylvania State University, University Park, PA 16802.

[1]L. Q. Chen and A. G. Khachaturyan, Phys. Rev. B **44**, 4681 (1991).

[2]L. Anthony and B. Fultz, J. Mater. Res. **4**, 1132 (1989).

[3]S. M. Allen and J. W. Cahn, Acta Metall. **24**, 425 (1976).

[4]A. G. Khachaturyan, T. F. Lindsey, and J. W. Morris, Jr., Metall. Trans. A **19**, 249 (1988).

[5]W. A. Soffa and D. E. Laughlin, Acta Metall. **37**, 3019 (1989).

[6]L. Q. Chen and A. G. Khachaturyan, Scr. Metall. Mater. **25**, 61 (1991); **25**, 67 (1991); Acta Metall. Mater. **39**, 2533 (1991).

[7]S. Matsumura, Y. Tanaka, K. Tankano, and K. Oki, in Proceedings of the International Workshop on Computational Materials Science, 1990, Tsukuba Science City, Japan (unpublished), pp. 231–234.

[8]K. Shiiyama, H. Kanemoto, H. Ninomiya, and T. Eguchi, Proceedings of the International Workshop on Computational Materials Science, 1990, Tsukuba Science City, Japan (unpublished), pp. 103–110.

[9]A. G. Khachaturyan, Fiz. Tverd. Tela (Leningrad) **9**, 2594 (1967) [Sov. Phys. Solid State **9**, 2040 (1968)]; *Theory of Structural Transformations in Solids* (Wiley, New York, 1983).

[10]J. W. Cahn and J. E. Hilliard, J. Chem. Phys. **28**, 258 (1958).

[11]A. G. Khachaturyan, Phys. Met. Metallogr. **13**, 493 (1962); Fiz. Tverd. Tela (Leningrad) **5**, 26 (1963) [Sov. Phys. Solid State **5**, 16 (1963)]; **5**, 750 (1963) [**5**, 548 (1963)]; Phys. Status Solidi B **60**, 19 (1973).

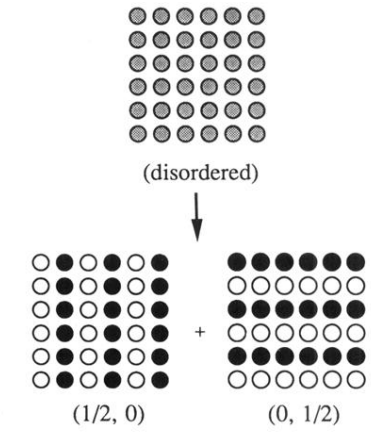

FIG. 1. Structures of a disordered state and two orientation variations of an ordered phase in a two-dimensional square lattice. $n(r)=1.0$ (solid circle), $n(r)=0.0$ (open circle), and $n(r)=0.5$ (grey circle).

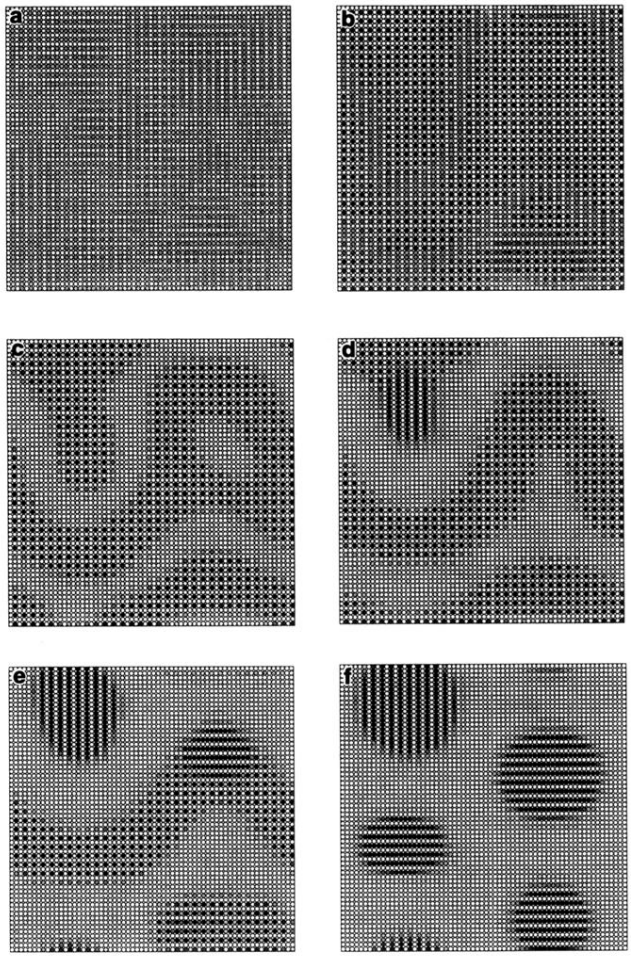

FIG. 3. Temporal evolution of the atomic structures and morphologies for a disordered solution of composition 0.175 aged at the temperature $T^*=0.10$ within the equilibrium two-phase field at different reduced time t^*. Each picture is a $64a \times 64a$ supercell. The grey levels of the circles represent the occupation probabilities of solute atoms at each lattice site. Complete dark means that the occupation probability is 1.0, while the complete bright means that the occupation probability is 0. All the intermediate grey levels indicate the occupation probabilities between 0 and 1. (a) $t^*=4.0$, (b) $t^*=15.0$, (c) $t^*=100.0$, (d) $t^*=300.0$, (e) $t^*=500.0$, and (f) $t^*=950.0$.

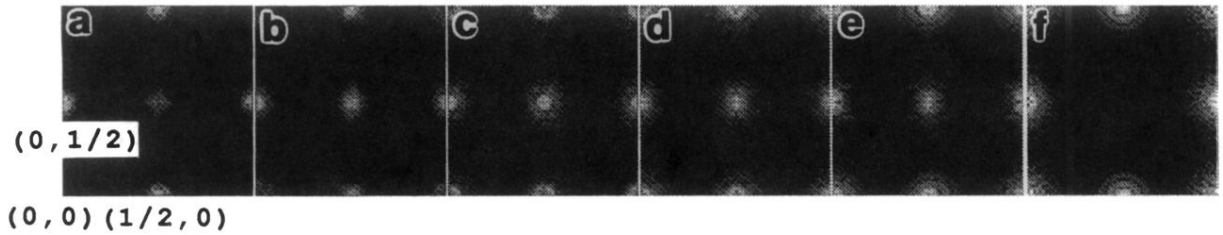

FIG. 4. Temporal evolution of the diffraction intensities within the first Brillouin zone calculated from the atomic structures presented in Fig. 3. Intensities of superlattice reflections are represented by the brightness, with the intensity of the fundamental reflection at the reciprocal-lattice origin (0,0) omitted.

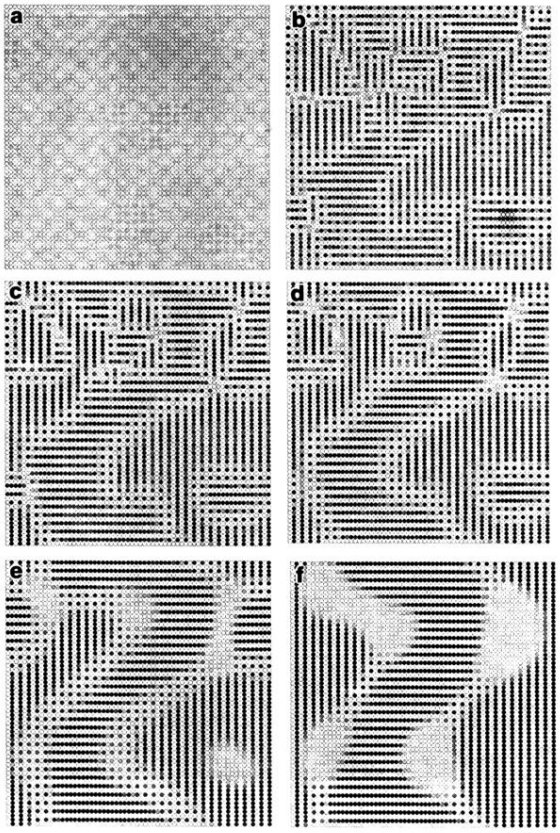

FIG. 7. Temporal evolution of the atomic structures and morphologies for a disordered solution of composition 0.35 aged at the temperature $T^*=0.10$ within the equilibrium two-phase field. (a) $t^*=2.0$, (b) $t^*=5.0$, (c) $t^*=50.0$, (d) $t^*=100.0$, (e) $t^*=305.0$, and (f) $t^*=605.0$.

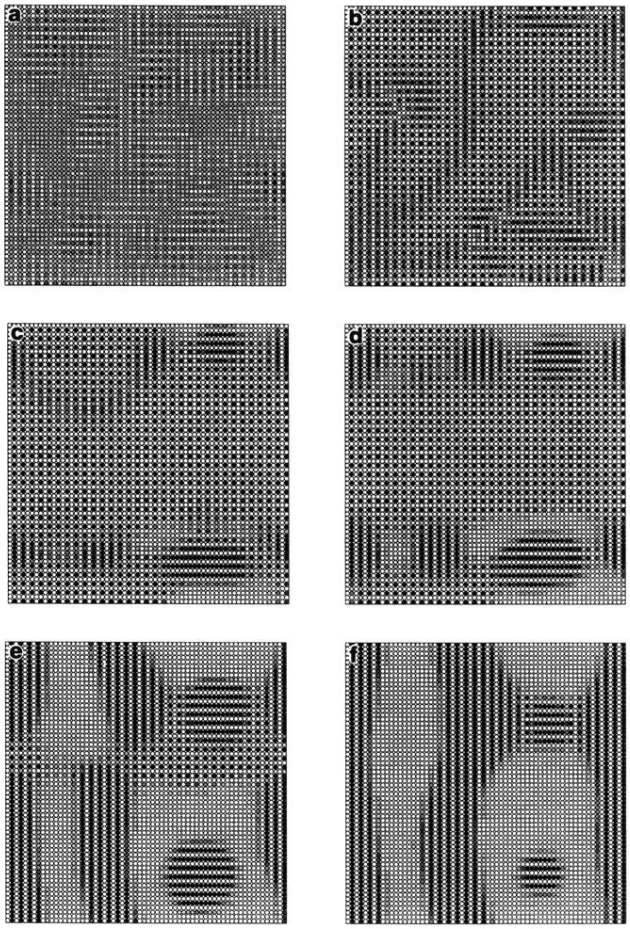

FIG. 8. Temporal evolution of the atomic structures and morphologies for a disordered solution with a composition corresponding to the stoichiometric composition of the virtual ordered phase, aged at the temperature $T^*=0.10$ within the equilibrium two-phase field. (a) $t^*=1.0$, (b) $t^*=2.0$, (c) $t^*=5.0$, (d) $t^*=10.0$, (e) $t^*=50.0$, and (f) $t^*=300.0$.